Volume 27 S, 2018

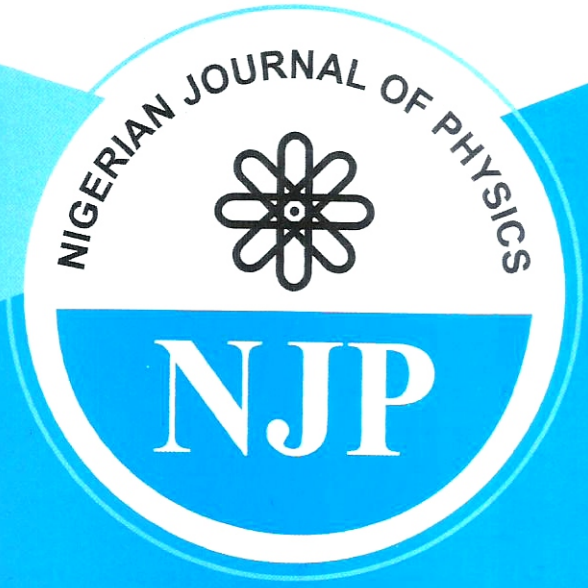

ISSN: 1595 - 0611

NIGERIAN JOURNAL OF PHYSICS

Published by
Nigerian Institute of Physics
Website: www.nipngn.org

CONTENTS

SYNTHESIS AND CHARACTERISATION OF PLATINUM DOPED MULTIWALL CARBON NANOTUBE

Ibrahim S. O.[1*], Isah, K. U.[1], Abdulkareem A. S.[2], Ahmadu U.[1]

[1]*Department of Physics, Federal University of Technology, Minna, Nigeria*
[2]*Department of Chemical Engineering, Federal university of Technology, Minna, Nigeria*
[1]*sharifat.ibr@futmina.edu.ng,* [1]*kasim309@futminna.edu.ng,* [2]*kasaka2003@futminna.edu.ng,*
**Corresponding author:* [1]*umaruahmadu@futminna.edu.ng.*

Abstract

Carbon nanotubes (CNTs) were synthesised by catalytic chemical vapour deposition (CCVD) method. The synthesised CNTs was purified by acid (H_2SO_4 and HNO_3) treatment to improve metal deposition on to CNTs surface. Platinum multiwall (Pt-MWCNTs) nanocomposites were then produced by wet impregnation of the platinum onto the surface of the MWCNTs. Surface morphology, chemical composition and crystallographic structure of the obtained Pt-MWCNTs nanocomposites were confirmed by Scanning Electron Microscopy (SEM), Transmission Electron Microscopy (TEM), Energy Dispersive X-ray spectroscopy (EDS), X-ray Diffraction (XRD) and Brunauer-Emmett-Teller (BET).

Keywords: *Catalytic Chemical Vapour Deposition (CCVD), Pt, X-ray Diffraction (XRD)*

1.0 INTRODUCTION

Since the discovery of carbon nanotubes by Iijima in 1991, during the synthesis of fullerenes by arc discharge, (Iijima, 1992), carbon nanotubes (CNTs) have become one of the headlines of nanotechnology as a result of their fascinating properties that have contributed to various applications such as energy storage materials, polymer reinforcements, gas storage materials, sensors, electronics and catalysis (Yibo, *et al.,* 2015; Zhang, *et al.,* 2013; Schnorr, *et al.,* 2011). These applications of carbon nanotubes can be developed on a large scale only if CNTs are controllably assembled into more sophisticated and hierarchical architectures as well as joined with other materials (Pawlyta, *et al.,* 2012). For this reason, it is extremely important to study and investigate effects of covering carbon nanotubes surface with metal and semiconductor nanoparticles (Pawlyta, *et al.,* 2012). Nanocomposites, obtained as result of the process may be a valuable material because of combination of unique physical and chemical properties of the components such as large surface area of CNTs and high conductivity of CNT and platinum (Lukowiec, *et al.,* 2013: Stobrawa, *et al.,* 2007: Wildgoose, *et al.,* 2006). Both components are characterised by large specific surface area and high value of electric conductivity. It was confirmed (Punbusayakul, 2013: Kong, *et al.,* 2000) that carbon nanotubes conductivity changed as a result of the interaction with molecules of many chemical substances, both liquids and gases. That effect is even more distinct after covering the carbon nanotubes surface with noble metals such as Au, Pt, Pd (Pawlyta, *et*

al., 2012). Platinum is an important raw material with many applications such as catalyst for CO oxidation in catalytic converters, fuel cell technology and as stable electrode material in solar cell fabrication (Pawlyta, *et al.,* 2012; Sharma, & Pollet, 2012; Antolini, Salgado, & Gonzalez, 2006). Due to these fantastic applications there is need to increase its effectiveness for uses especially as nanocrystals. Since decrease in nanocrystal diameter results in increase in specific surface area and size of nanocrystals are connected with specific surface area. In addition, Platinum is an expensive material, if this is to employed for large scale application, quantity of platinum required in applied processes has to be reduced to bring down the cost of product which would lower the market price of the final product, thus, there is need for Pt-MWCNTs.

This work presents the synthesis of nanocomposite consisting of CNTs coated with platinum nanoparticles and investigate the effect of deposition time on the quantity of platinum deposited on CNTs. The CNTs was synthesised via catalytic vapour deposition technique. The CNTs nanocomposites were prepared by deposition of platinum nanoparticles on the CNTs.

The samples were characterised using UV-VIS Spectroscopy, scanning electron microscopy (SEM), transmission electron microscopy (TEM), Brunauer-Emmett-Teller (BET) and X-ray structure analysis (XRD).

2.0 EXPERIMENTAL

2.1: Preparation of Catalysts

2.1.1: *Wet Impregnation*

All the chemicals used in this study were of analytical grade with percentage purity in the range of 98% – 99.99%. The catalyst used for growing the CNTs in this study was prepared using Fe and Co metals supported on $CaCO_3$. Wet impregnation method was used for the synthesis of the catalysts, this is a linear multistep process that involved pre-calcination and calcination treatments. The bimetallic catalyst Fe-Co on $CaCO_3$ support was prepared as described by Afolabi, *et al.,* (2011), which is targeted mainly at dispersing the Fe and Co active components into the pores of the $CaCO_3$ surface so as to be available to reactant (acetylene). A known weight of this catalyst, which contained equal proportion by weight of iron and cobalt was prepared by dissolving 2.47 g mass of $Co(NO_3)_2.6H_2O$ (Kem Light Lab., Mumbai India, 98.5%) and 3.62 g mass of $Fe(NO_3)_3.9H_2O$ (Guangdong Guanghua Chemical Factory Co., Ltd, China, 98.5) in 50 mL distilled water to make Fe-Co precursor solution. 10g of $CaCO_3$ (Kermel, China) was then added to the mixture and allowed to age for 60 minutes under constant stirring on magnetic stirrer until it become a gel. The resulting gel was then baked at 120°C for 12 hours and then cooled to room temperature. After cooling to room temperature, the residuals were grounded and screened through 150 µm sieve into fine powder. The resulting powder was then calcined at temperature 400°C for period of 16 hours in a furnace. The dried catalyst-substrate mixture was grounded to avoid any agglomeration that may affect the interaction between carbon source and the surface of the mixture.

The yields of the bi-metallic catalysts prepared were calculated after oven-drying ($Yield_{(oven-drying)}$) and after calcination ($Yield_{(calcined)}$) according to Equations (1) and (2), and the calculated yields after oven-drying and calcination, are presented in Table (2).

$$Yield_{(oven-drying)}(\%) = \frac{Mass\ of\ catalysts\ after\ oven-drying}{Mass\ of\ the\ mixture} \times 100\% \quad (1)$$

$$Yield_{calcined}(\%) = \frac{Mass\ of\ catalysts\ after\ calcination}{Mass\ of\ catalysts\ after\ oven-dring} \times 100\% \quad (2)$$

The catalysts produced was analysed to determine the morphology, elemental composition, crystallinity and thermal stability using SEM, EDX, XRD and TGA respectively and this was then used for the carbon nanotube production.

The catalysts produced were used for synthesis of CNTs.

2.2 Synthesis of Carbon Nanotube

Carbon nanotubes were grown using chemical vapour deposition (CVD) techniques. Figure 1 shows the schematic set up and working of the CVD system. The bi-metallic Fe-Co catalyst on $CaCO_3$ support (0.5 g) was spread to form a thin layer in a ceramic boat, (e) and the boat was then placed horizontally in the centre of the quartz tube, (d).

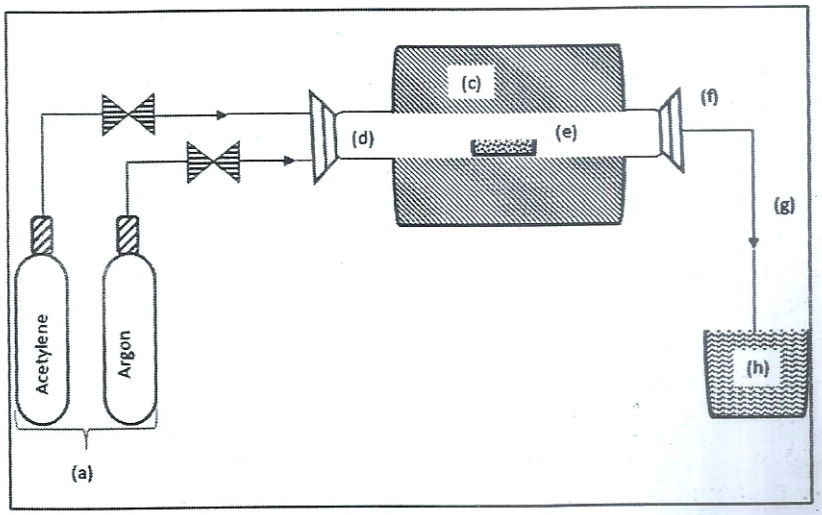

Figure 1: Schematic diagram of experimental set-up for CNT synthesis in CVD

Heating ramping rate was set at 10 °C/ min and argon was set to flow over the catalyst at the rate of 30 ml min^{-1} to purge the system off air. Once the set temperature, 700 °C was attained, the argon flow was adjusted to the required flow rate (190 ml min^{-1}) and acetylene was introduced at its required flow rate (290 ml min^{-1}). This process continued until the reaction time (60 min) was reached after which the flow of acetylene was discontinued. The furnace was allowed to cool down to room temperature under continuous flow of argon at 30 ml min^{-1}. The ceramic boat was then removed and weighed to determine the quantity of CNTs produced. Percentage of CNTs yield was determined using the relationship provided by (Yeoh, *et al.*, 2009; Taleshi, 2012) as presented in Equation (3):

$$Carbon\ yeild = \frac{(weight\ of\ carbon\ deposited) - (weight\ of\ catalyst\ used)}{(weight\ of\ catalyst\ used)} \times 100\% \quad (3)$$

2.3 Purification of Carbon Nanotubes (CNTs)

The as-synthesised carbon nanotubes were pre-treated with a mixture of concentrated H_2SO_4 and HNO_3 {Guangdong Guanghua Sci-Tech Co., Ltd (JHD), (3: 1 by volume)}. This acid mixture was vigorously stirred with the carbon nanotube samples for 3 hours at 45 °C in the sonicator to remove the metallic impurities as well as functionalise the surfaces of the carbon nanotubes to enhance metal dispersion. This mixture was then washed thoroughly with distilled water until a pH of 7 was achieved. These functionalised carbon nanotube samples were then dried in oven at 120 °C for 12 hours.

2.4 Preparation of Pt-MWCNT

A known amount of purified MWCNTs (1g) was placed in a 50ml glass beaker, mixed with 30 ml five percent (5%) polyethylene glycol (PEG). The mixture was subjected to agitation in a sonic bath at room temperature for 30 minutes, then magnetically stirred under reflux for a period of 4 hrs at room temperature, after which 10 ml of potassium tetra-chloroplatinate (K_2PtCl_4) solution (0.01M) was introduced into mixture of polyethylene glycol and MWCNTs. The mixture was then stirred for a period of 30 min more to form a homogenous suspension after which it was then filtered to separate the residue and the filtrate from one another. The residue was then air dry at room temperature overnight and at a temperature of 120 °C for 12 hrs in the oven. The oven dried samples were calcined at 300 °C for 16 hrs. The calcined Pt-MWCNT composite was then pulverised with a mortar and pesstle and then sieved with a 212 µm mesh. The procedures were repeated for 60, 90, 120, 150, 180, 210 and 240 min. The filtrate collected was analysed from the absorbance profile using a scanning spectroscopy UV1800 series to determine the absorbance of platinate salt at a specific platinum wavelength of 214 nm and distilled water was used as a blank. Bear's Law was used to estimate the concentration of filtrate and the result was then used to calculate the concentration of the platinum deposited on the CNTs. This concentration was estimated by subtracting the concentration of filtrate from the concentration of platinum stock solution (4.17 gdm^{-3}). The difference been the concentration of the platinum deposited on the CNTs which was later converted into percentage concentration. Samples were labelled A270 to A480 according to deposition time.

2.5 Characterisation

The Nanocomposites synthesised were characterised for percentage concentration of Pt nanoparticles on CNTs using (UV Spectroscopy), the morphology by Scanning electron microscope (SEM), transmission electron microscopy (TEM/EDX), its crystallinity using X-Ray diffraction (XRD) and surface area by Brunauer-Emmett-Teller (BET).

3. RESULTS AND DISCUSSIONS

3.1 Scanning Electron Microscopy (SEM) Analysis of the Catalyst sample

The SEM micrographs (Figure. 2a) revealed the presence of clustered solid catalyst material, scattered on the Fe-Co/$CaCO_3$ composite. The micrographs presented in Figure. 2b further revealed that the catalyst produced exhibited well distributed nano-flakes grown on the substrate surface ($CaCO_3$). SEM micrograph also show micro-pores in the catalyst, a property indicating that there

was proper dispersion of Fe and Co nanoparticles on the $CaCO_3$ support material with minute spaces within the composite. The $CaCO_3$ matrix sites were uniformly occupied by the oxides of Fe and Co that were formed during calcination of the catalyst sample. The random arrangement of the nano-flakes as revealed by the SEM micrograph indicated that the sample surface is highly porous, which is an important prerequisite material for production of CNT.

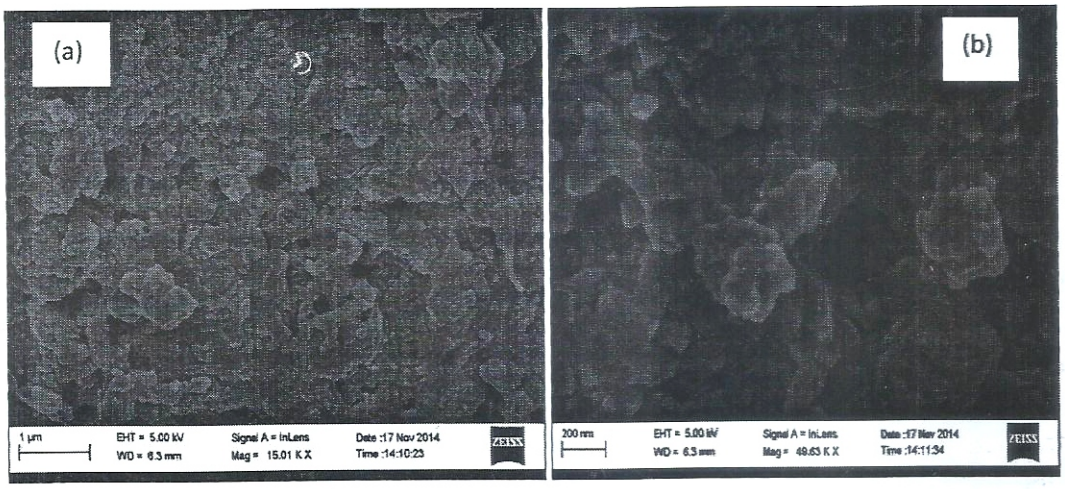

Figure 2: SEM image showing nanoparticles of Fe and Co dispersed on $CaCO_3$ support

3.2 SEM/EDX of the Catalyst

Figure 3 is the SEM/EDS analysis of the synthesised catalyst. The spectrum qualitatively confirmed presence of Fe, Co, Ca, C and O which are chemical components of the catalyst. The presence of oxygen in the sample could be attributed to the presence of oxygen in the support ($CaCO_3$) and conversion of Fe and Co metals into their respective oxides during calcination.

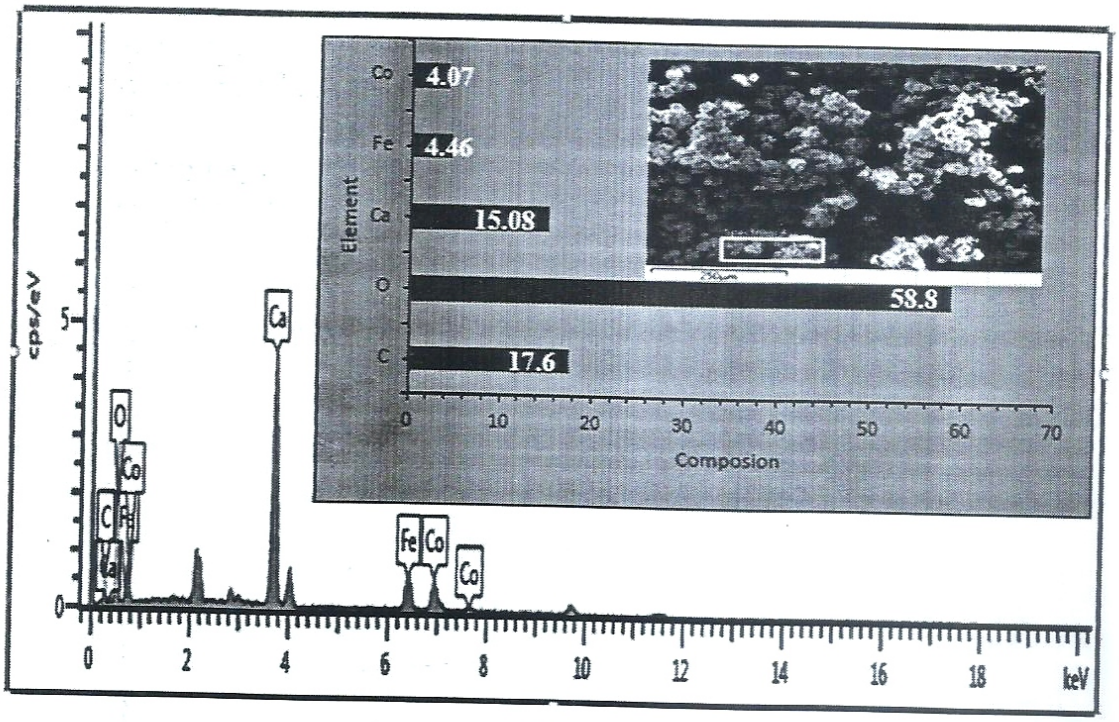

Figure 3: SEM/EDS image of Fe-Co/$CaCO_3$ catalyst sample after calcination

3.3 X-Ray diffraction (XRD) of the Catalyst

Figure 4 is the XRD pattern showed that the solid catalyst is polycrystalline, with different crystal sizes ranging from 39.6 nm to 79.4 nm that result in a number of peaks which were attributed to be $CaCO_3$ and $CoFe_2O_4$ phases as indicated in the Figure.

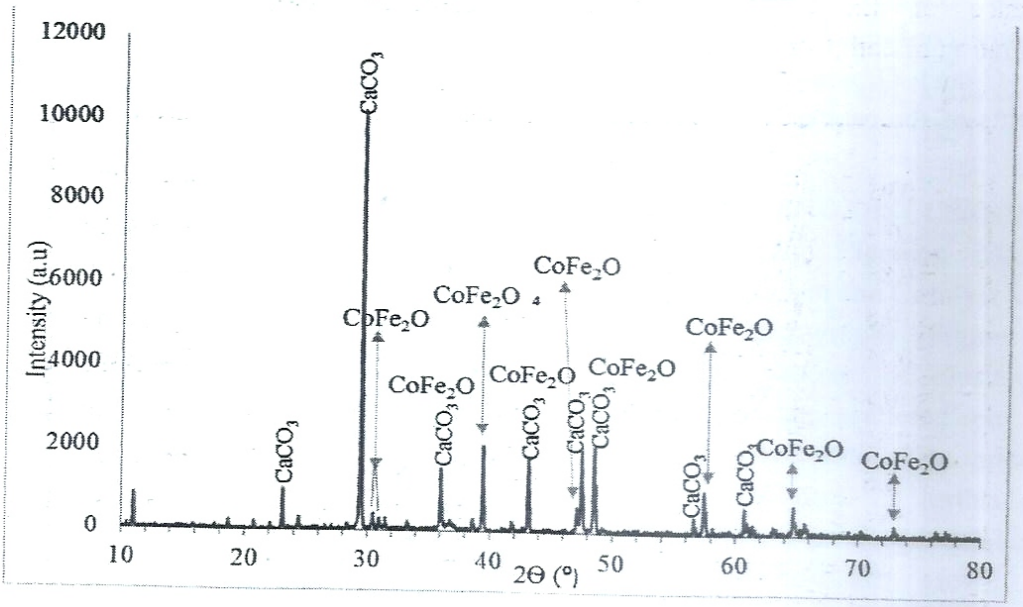

Figure 4: XRD pattern of Fe-Co/$CaCO_3$ catalyst

3.4 Thermogravimetric analysis (TGA)

Figure 5 is the TGA profile of the catalyst conducted in nitrogen environment showing how the catalyst decomposed thermally at four different regimes. The first slope is attributed to loss of unbound water, the next two weight losses are due to conversion of Fe and Co nitrates to form a ternary metal oxide, most likely, $CoFe_2O_4$. The final weight loss represents the decomposition of $CaCO_3$ to evolve CO_2 and form CaO.

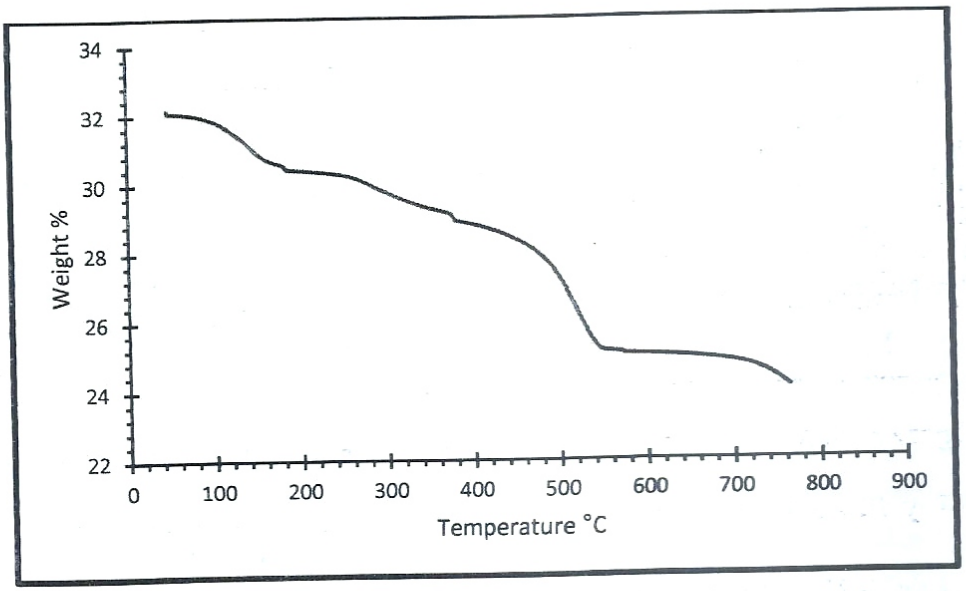

Figure 5: TGA curve of Fe-Co/$CaCO_3$

3.1 UV-vs Spectroscopy

The UV spectroscopy results of absorbance of filtrate and estimated concentration of both filtrate and CNTs are presented in Figure 6. Sample A270 with lowest deposition time had the highest absorbance peak.

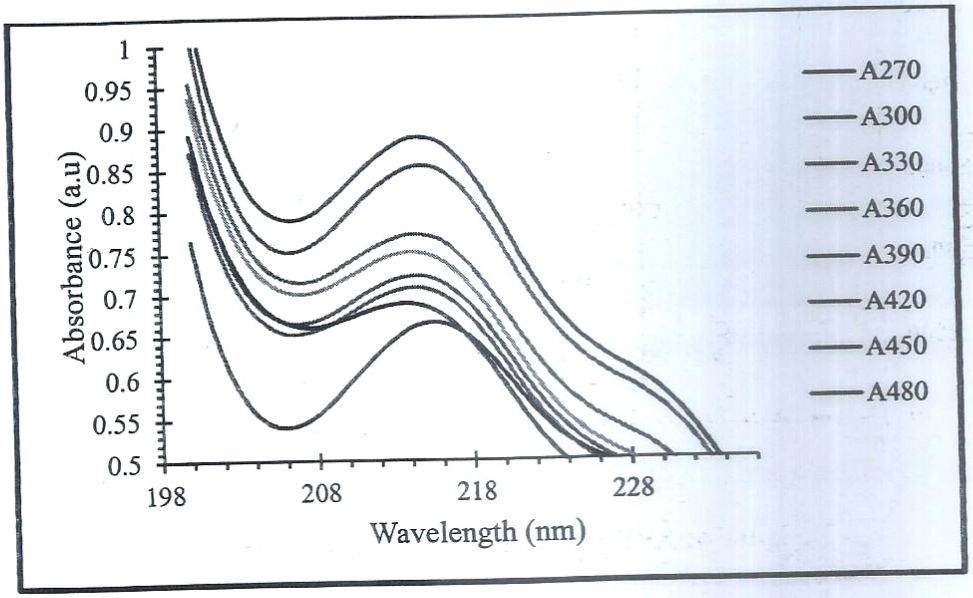

Figure 6: Combined plots of UV Spectrum of Pt left inside the filtrate.

Figure 6: presented the Combined plots of UV Spectrum of Pt left inside the filtrate. Each of the spectral represent experiment run for a particular deposition time, from 270 mins to 480 mins.

Table 1 shows the percentage concentration of Pt on CNTs based on time of deposition. The result shows that the absorbance of the filtrate decreases with increased in deposition time. The filtrate concentration decreases with absorbance of the filtrate while the concentration of Pt-MWCNTs increases with the filtrate absorbance. Bear Lambert law was used to estimate the concentration of Pt in the filtrate and the concentration of Pt on MWCNT was extrapolated from this. The concentration of Pt-MWCNTs was determined by subtracting the concentration of filtrate from the concentration of the Pt stock solution. since it value is the deference between concentrations of platinum stock solution and filtrate. The sample with longest deposition time 480 mins had the highest % concentration of Pt on CNTs.

Table 1: UV-vs analysis showing Pt percentage concentration on CNTs

Sample ID	Deposition time (mins)	Absorbance of filtrate (a.u)	Filtrate Concentration	Concentration of Pt on CNTs	% Concentration of Pt on CNTs
A270	270	0.887	3.52	0.65	15.54
A300	300	0.854	3.37	0.79	19.05
A330	330	0.772	3.01	1.16	27.79
A360	360	0.751	2.92	1.25	30.03
A390	390	0.722	2.79	1.38	33.12
A420	420	0.708	2.72	1.44	34.62
A450	450	0.689	2.64	1.53	36.64
A480	480	0.665	2.53	1.63	39.20
A510	510	No formation	No formation	No formation	No formation

3.2 Scanning Electron Microscopy (SEM) of Pt-MWCNTs

Figure 7 is SEM micrograph images (a) of CNTs and that (b) of Pt-MWCNTs composite. Results as presented indicates that the morphology of the samples changes from smooth as observed from SEM micrograph of CNTs to rough surface for Pt-MWCNTs nanocomposites.

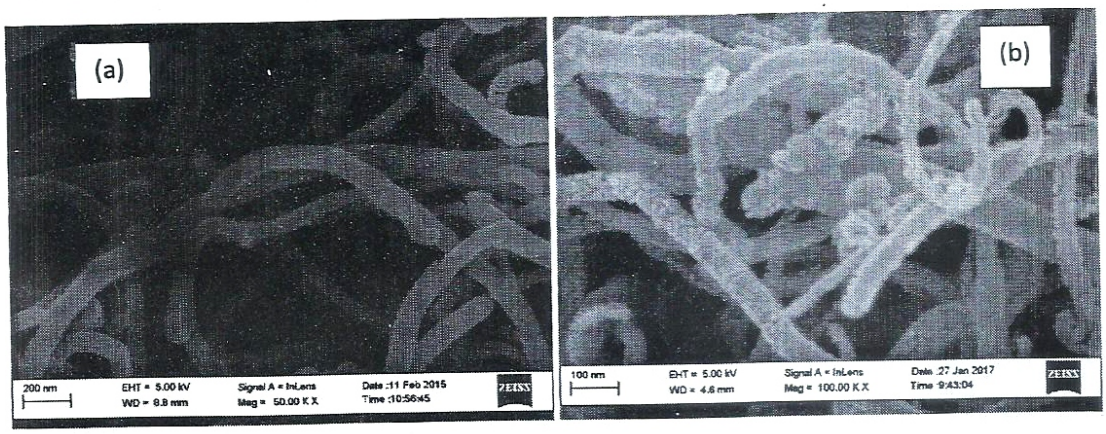

Figure 7: SEM Images (a) of purified CNTs and (b) Pt-CNTs Showing Effect of Pt on CNTs.

3.3 Transmission Electron Microscope (TEM).

Figures 8: is the TEM images of CNTs doped with platinum nanoparticles, (a) shows that the CNTs produced is a multiwall and the dark spots (b) on the matrices of MWCNTs are platinum particles. It further showed that these particles are adsorbed on the surface of the CNTs. Observed particles appear to have a narrow size distribution, and no free particles were observed in the background of the TEM images, which confirms all formed platinum nanoparticles were attached to the nanotubes wall. The images show these particles are well–dispersed and homogeneously anchored on the surface of the CNTs

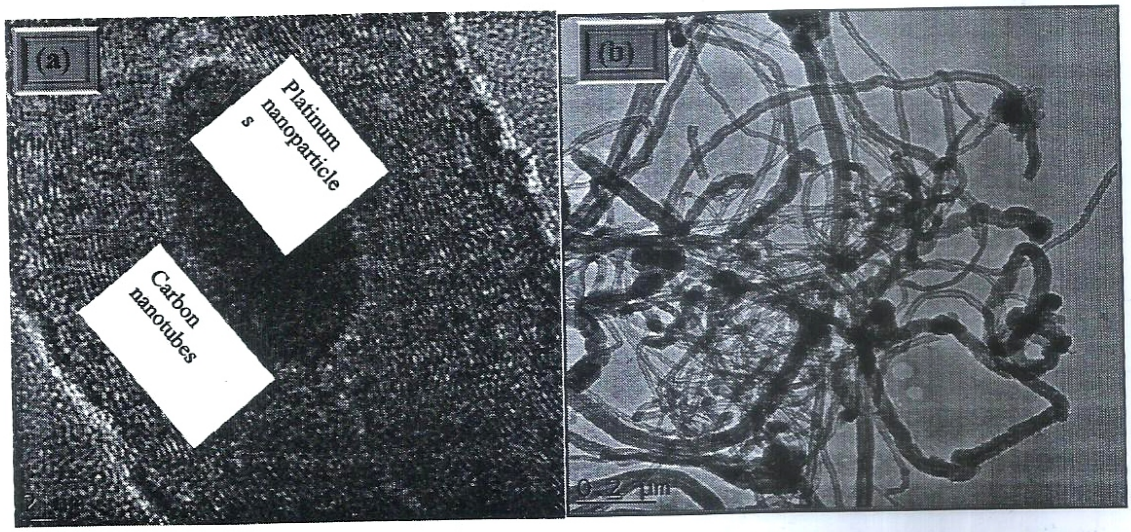

Figure 8: (a) showing evidence of multiple walls and Pt. catalyst on the nanotube, (b) Pt nanoparticles evenly distributed on the outer surface of the tubes.

The combine TEM spectrum and EDS are shown in Figure 9 confirm the presence of Pt, however, also detected are C, O, Fe and Ca atoms from catalyst used for synthesis of CNTs.

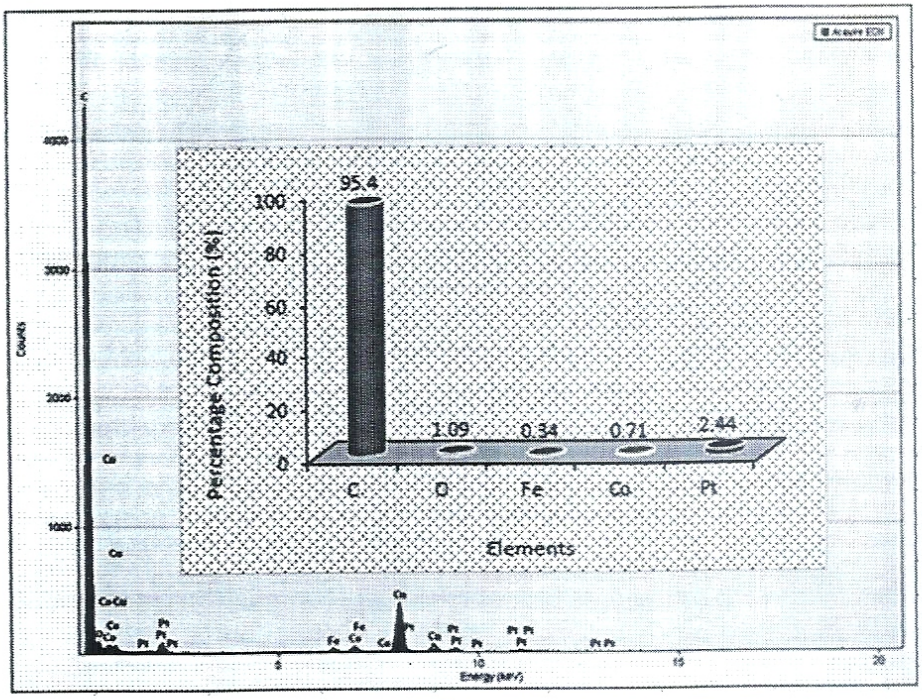

Figure 9: TEM/EDS of the Pt–MWCNT catalyst sample confirming the presence of Pt.

3.4 XRD analysis of Pt–MWCNT catalysts

Figure 10 is the XRD pattern for Pt-MWCNTs catalyst, which shows the diffraction peaks at $2\theta = 25.92^{0}$C, 44.68^{0}C and 53.84^{0}C that can be attributed to the graphitic (002), (101) and (004) planes of the CNTs, while other peaks at 39.60^{0}C, 67.83^{0}C and 82.45^{0}C identify the characteristic face centred cubic (fcc) structure of crystalline platinum planes of Pt at (111), Pt (220), Pt (311), respectively.

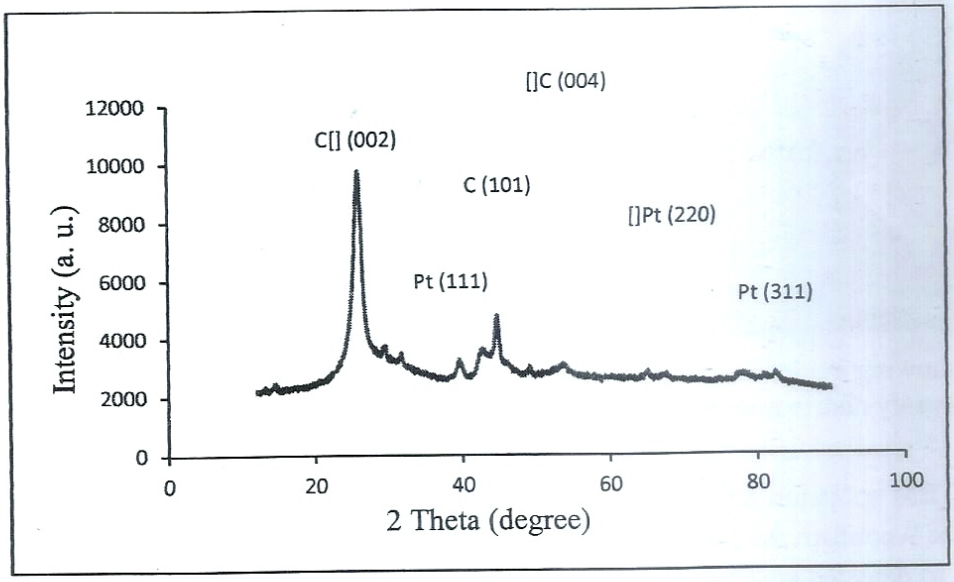

Figure 10: XRD pattern of Pt–MWCNT catalyst sample

This indicates that Pt nanoparticles are composed of pure crystalline Pt since no other peaks are observed in the XRD patterns (Yang *et al.,* 2016: Lukowiec, 2013). This is an indication that the platinum precursor employed (K_2PtCl_4) in this study has been reduced to metallic platinum (Bayrakceken *et al.,* 2008). The lattice parameters "a" of platinum as revealed by XRD is 3.90129 Å which corresponds to the literature (Katarzyna *et al.,* 2015; Foiles *et al.,* 1986; Wheeler, 1925) value 3.92310 Å. The average crystallite size of Pt deposited on MWCNTs support was evaluated using the relationship presented in Scherrer's equation as given in Equation (1).

$$D = \frac{K\lambda}{\beta cos\theta} \quad (1)$$

where

D = the average crystalline size of the platinum particles

K = the Scherrer constant = 0.94

λ = the wavelength of X–ray radiation which is equal to 1.54051Å (0.154051nm).

β = the full width at half – maximum (FWHM) of the (111, 220 and 311) diffraction line.

θ = the Bragg angle measured in radians at the position of platinum peaks

The evaluation of crystallite size of Pt particle was estimated from the diffraction peaks Pt (111), Pt (220) and Pt (311) and the evaluated sizes was found to be 1.35 nm, 7.77 nm and 8.80 nm respectively, with an average size of 6.0 nm. The major diffraction peak was found to be Pt (111) at 2theta of 39.60. The diffraction peak, Pt (111) at 2theta of 39.60 with crystal size 1.35 nm can be regarded as the strongest Pt peak.

3.5 Brunauer-Emmett-Teller (BET) Analysis of Purified and Pt–CNT catalysts

The influence of deposition concentration on the surface area and pore volume of the Pt-MWCNTs composite was investigated by BET the results obtained is as shown in Table 2. The results as presented indicated that the surface area and pore volume of the samples increases as the percentage concentration of platinum nanoparticles increases on the surface of the CNTs.

Functionalisation and metals, influences the specific surface area of nanotubes (Birch *et al.,* 2013; Naseh *et al.,* 2009), since functionalisation causes opening up tube ends (Tsang *et al.,*1994) and generation of defects on the sidewall of nanotubes (Banerjee *etal.,*2005), therefore access into the cavity of the nanotubes can be achieved. Therefore, the increase in the surface area and pore volume observed can then be attributed to the surface functionalisation and presence of Pt nanoparticles deposited on the surface of the sample. Result as presented indicate that the higher the concentration of the metal nanoparticles the higher the specific surface area.

Table 2: BET analysis of Pt-MWCNTs catalyst samples

Pt concentration on MWCNTs.	Surface area (m^2g^{-1})	Pore volume (cm^3g^{-1})
Purified	274.06	62.97
33.12 wt% Pt.	432.6	19.14
34.62 wt% Pt.	609.2	26.82
39.20 wt% Pt.	858.7	38.82

4. CONCLUSIONS

Pt-MWCNTs nanocomposites were synthesised by coating Pt on MWCNTs produced by catalytic chemical vapour deposition. The analysis carried out using scanning electron microscopy and transmission electron microscopy analysis has confirmed that CNTs produced is a MWCNTs and after deposition process, nanocomposites were obtained and that this composed of MWCNTs coated with nanoparticles with small weight fraction of Pt as revealed by UV spectroscopy. The results obtained from XRD clearly confirm a crystalline structure of the deposited nanoparticles of precious metals with sizes ranging from 1.35 to 8.80 nm and quantity of the nanoparticles impregnated on the surface of CNTs is based on the time of deposition. BET also confirmed that presence of this noble metal on the surface of CNTs increases its specific surface area of the nanocomposites also this increase depends on the quantity of nanoparticles deposited on the surface, it increases linearly with quantity deposited. The difference identified is directly related to a higher number of defects in a graphite structure of CNTs coated with platinum nanoparticles as a result of functionalizing their surface with a mixture of acids.

REFERENCES

Afolabi, A. S. (2009). Development of carbon nanotubes platinum electro catalytic electrodes for proton exchange membrane fuel cell. Unpublished PhD thesis, *University of the Witwatersrand, Faculty of Engineering and the Built Environment. Johannesburg, South Africa,* 65-80.

Antolini, E., Salgado, J. R. C. & Gonzalez, E. R. (2006). The stability of Pt-M (M = first row transition metal) alloy catalysts and its effect on the activity in low temperature fuel cells – A literature review and tests on a Pt-Co catalyst. *J. Power Sources* **160,** 957–968.

Banerjee, S., Hemraj T. and Wong, S., (2005). "Covalent surface chemistry of single-walled carbon nanotubes". *Advance. Materials,* 1, 17.

Bayrakçeken, A., Erkan, S. A., Turker, L. and Eroglu, I., (2008). Effects of membrane electrode assembly components on proton exchange membrane fuel cell performance. *International Journal of Hydrogen Energy*, 33, 165-170.

Birch, E. M., Ruda-Eberenz, T. A., Chai, M., Andrews, R. and Hatfield, R. L., (2013). Properties that Influence the Specific Surface Areas of Carbon Nanotubes and Nanofibers. *Annals of Occupational Hygiene* 57(9), 1148-1166. doi:10.1093/annhyg/met042.

Foiles, S. M., Baskes, M. I. and Daw, M. S., (1986). Embedded-atom-method functions for the *fcc* metals Cu, Ag, Au, Ni, Pd, Pt, and their alloys. *Physical Review B 33*, 7983-7991.

Iijima, S. (1991). Helical Microtubules of GraphiticHelical Microtubules of Graphitic Carbon. *Nature,,* 354, 56-58. doi:10.1038/354056a0.

Ijima, S. A. (1992). Growth model for carbon nanotubes. Physical Peview Letters, *69(21),* 3100-3103.

Katarzyna K., Marco M., Paweł J., Tomasz K. and Aleksander K., (2015). Structure Determination of Au on Pt (111) Surface: LEED, STM and DFT Study. *Materials* 8, 2935-2952; doi: 10.3390/ma806293

Kong, J., Franklin, N. R., Zhou, C., Chapline, M. G., Peng, S., Cho, K. and Dai, H., (2000). Nanotube Molecular Wires as Chemical Sensors *Science,* 287, 622-625.

Kong, J., Franklin, N. R., Zhou, C., Chapline, M. G., Peng, S., Cho, K. and Dai, H., (2000). Nanotube Molecular Wires as Chemical Sensors *Science,* 287, 622-625.

Lukowiec, D., (2013). Synthesis and characterisation of Pt/MWCNTs nanocomposites. *Physical. Status Solidi B,* 1–6. DOI 10.1002/pssb.201300083

Naseh, M. V., Khodadadi, A. A., Mortazavi, Y., Sahraei, O. A., Pourfayaz, F. and Sedghi, S. M., (2009a). Functionalization of Carbon Nanotubes Using Nitric Acid Oxidation and DBD Plasma. *International Journal of Chemical, Molecular, Nuclear, Materials and Metallurgical Engineering,* 3 (1), 33-35.

Pawlyta, M., Łukowiec, D. and Dobrzańska-Danikiewicz, A. D., (2012). Characterisation of carbon nanotubes decorated with platinum nanoparticles. *Journal of Acheivement in materials and manufacturing Enginneering,* 53(2), 67-75.

Punbusayakul, N., (2012). Carbon nanotubes architectures in electro analysis. *Science Direct* Procedia Engineering, 32, 683-689.

Punbusayakul, N., (2012). Carbon nanotubes architectures in electro analysis. *Science Direct* Procedia Engineering, 32, 683-689

Schnorr, J. M. (2011). Emerging Applications of Carbon Nanotubes. *Chemistry of Materials: American Chemical Society,* 23, 646-57.

Sharma, S. & Pollet, B. G. (2012). Support materials for PEMFC and DMFC electro catalysts-A review. *J. Power Sources* 208, 96−119, doi: 10.1016/j.jpowsour.2012.02.011.

Stobrawa, J. P., Rdzawski, Z. M. and Głuchowski, W. J., (2007). Microstructure and properties of anocrystalline copper-yttria micro-composites. *Journal of Achievements in Materials and Manufacturing Engineering,* 24(2), 83-86.

Stobrawa, J. P., Rdzawski, Z. M. and Głuchowski, W. J., (2007). Microstructure and properties of nanocrystalline copper-yttria microcomposites. *Journal of Achievements in Materials and Manufacturing Engineering,* 24(2), 83-86.

Taleshi, F. (2012), "Evaluation of new processes to achieve a high yield of carbon nanotubes by CVD method". *International Nano Letters,* 2(23), pp. 1-5.

Wheeler, D., (1925). Precision measurements of the lattice constants of twelve common metals. *Physical Review,* 25, 753-761. Doi: 10.1103/Phys/Rev. 25, 753.

Wildgoose, G. G., Banks, C. E., Compton, R. G., (2006). Metal nanoparticles and related materials supported on carbon nanotubes: methods and applications. *Small* 2(2), 182 - 193.

Wildgoose, G. G., Banks, C. E., Compton, R. G., (2006). Metal nanoparticles and related materials supported on carbon nanotubes: methods and applications. *Small* 2 (2), 182-193.

Yang, X. Z. (2016). Effect of carbon nanotube (CNT) content on the properties of in-situ synthesis CNT reinforced Al composites. Mater Sci Eng A, 660, 11 (2016).http://www.sciencedirect.com/science/article/pii/S0921509316301745

Yeoh, W. M., Lee, K. Y., Chai, S. P., Lee, K. T., & Mohamed, A. R. (2009), Synthesis of high purity multi-walled carbon nanotubes over Co-Mo/MgO catalyst by the catalytic chemical vapour deposition of methane. *New Carbon Materials,* vol. 24(2), pp. 119 – 123

Yibo, Y. J.-X. (2015). Carbon nanotube catalysts: recent advances in synthesis, characterization and applications. doi:10.1039/c4cs00492b

Zhang, Q. H. (2013). The road for nanomaterials industry: a review of carbon nanotube production, post-treatment, and bulk applications for composites and energy storage. *Small,* 9(8), 1237-1265. doi:10.1002/smll.20120325